

Anomalous shift of the beating nodes in illumination-controlled $\text{In}_{1-x}\text{Ga}_x\text{As}/\text{In}_{1-y}\text{Al}_y\text{As}$ two-dimensional electron gases with strong spin-orbit interaction

W. Z. Zhou,^{1,2,3,*} T. Lin,³ L. Y. Shang,^{1,3} G. Yu,³ K. H. Gao,³ Y. M. Zhou,³ L. M. Wei,³ L. J. Cui,⁴ Y. P. Zeng,⁴ S. L. Guo,³ and J. H. Chu^{1,3,†}

¹Key Laboratory of Polar Materials and Devices, Ministry of Education, East China Normal University, Shanghai 200062, People's Republic of China

²College of Physics Science and Technology, Guangxi University, Nanning, Guangxi 530004, People's Republic of China

³National Laboratory for Infrared Physics, Shanghai Institute of Technical Physics, Chinese Academy of Sciences, Shanghai 200083, People's Republic of China

⁴Novel Materials Laboratory, Institute of Semiconductors, Chinese Academy of Sciences, Beijing 100083, People's Republic of China

(Received 21 October 2009; revised manuscript received 25 February 2010; published 11 May 2010)

The beating patterns in the Shubnikov-de Haas oscillatory magnetoresistance originating from zero-field spin splitting of two-dimensional electron gases (2DEGs) in $\text{In}_{0.52}\text{Al}_{0.48}\text{As}/\text{In}_x\text{Ga}_{1-x}\text{As}/\text{In}_{0.52}\text{Al}_{0.48}\text{As}$ quantum wells with silicon δ doped on the upper barrier layer have been investigated by means of magnetotransport measurements before and after illumination. Contrary to the expectation, after each illumination, the beating nodes induced by the zero-field spin-splitting effect shift to lower and lower magnetic field due to the decrease in the zero-field spin-splitting energy of the 2DEGs. The anomalous phenomenon of the shift of the beating nodes and the decrease in spin-orbit coupling constants after illumination cannot be explained by utilizing the previous linear Rashba model. It is suggested that the decrease in the zero-field spin-splitting energy and the spin-orbit coupling constant arise from the nonlinear Rashba spin splitting.

DOI: [10.1103/PhysRevB.81.195312](https://doi.org/10.1103/PhysRevB.81.195312)

PACS number(s): 73.21.Fg, 73.40.Kp, 71.70.Ej, 72.25.Rb

I. INTRODUCTION

Spin-orbit (SO) interaction, which is responsible for spin relaxation, is essential for the realization of various spintronic devices, e.g., spin-field-effect transistors^{1,2} or spin interferometers^{3–5} both in the diffusive region and ballistic region, spin filters,^{6,7} or spin splitters.⁸ The central theme of realization of such spintronic devices is to effectively control spin polarization, spin transport, and spin detection. However, much more difficult than originally anticipated, these devices have yet to be realized. The mechanisms for the SO interaction in semiconductors can originate from the Dresselhaus term induced by bulk inversion asymmetry (BIA) (Ref. 9) and/or the Rashba term induced by structural inversion asymmetry (SIA).^{10,11} The Rashba SO coupling is of particular interest due to its potential applications in spin field-effect transistor (SFET) in the ballistic region, as it can be controlled by an applied gate voltage.^{1,12–16} However, both Rashba and Dresselhaus spin splitting are required for fabricating nonballistic SFET.² For linear Rashba spin-relaxation mechanism, the electric field $\langle F \rangle$ due to band bending in the two-dimensional electron gas (2DEG) channel couples to the spin of electrons and the SO coupling constant α satisfies as $\alpha \propto \langle F \rangle$.^{12,17}

In III-V semiconductors, Rashba spin splitting is frequently considered as the main mechanism to the SO interaction in narrow gap materials such as InSb, InAs, InAs/GaSb, $\text{In}_x\text{Ga}_{1-x}\text{As}/\text{In}_y\text{Al}_{1-y}\text{As}$, or $\text{In}_x\text{Ga}_{1-x}\text{As}/\text{InP}$ theoretically or experimentally.^{17–22} Whereas, the Dresselhaus spin splitting is considered as dominant in wide gap materials such as $\text{Al}_x\text{Ga}_{1-x}\text{As}/\text{GaAs}$ theoretically.^{17,21} However, it was also shown that both SIA and BIA were of the important contribution to SO interaction even in the $\text{Al}_x\text{Ga}_{1-x}\text{As}/\text{GaAs}$ heterostructures.^{23–25}

In transport measurements, SO interaction and the associated spin splitting in zinc-blende III-V semiconductor heterostructures have been continuously studied for several decades.^{12–14,20,26–32} It is common to determine the SO coupling parameter from the beating pattern in Shubnikov-de Haas (SdH) oscillations^{12–14,20,26–29} or the analysis of weak antilocalization.^{28–32} For the former, the high electron-mobility system is required so that the SdH oscillations start to be visible in relatively low magnetic field and the beating nodes can be observed. When the III-V semiconductor quantum wells were controlled by applying a gate voltage on the top of the upper surface, both the carrier concentration and transport mobility show a continuously increase with increasing the gate voltage despite the carrier supplying layer upon or beneath the channel layer.^{12–14,29–32} Whereas, as the gate voltage increases from negative to positive, the pinning potential at the interface between the Schottky layer and the gate insulator will be shifted to a lower and lower potential position. Thus, if the linear Rashba mechanism is dominant, the strength of SO coupling constant α would be enhanced due to the increase in the potential gradient, i.e., the electric field $\langle F \rangle$, along the quantum well as the carrier supplying layer is upon the channel layer (sample 4 in Ref. 30, and samples 1 and 3 in Ref. 31), and be weakened due to the reduction in the potential gradient along the quantum well while the carrier supplying layer is beneath the channel layer (Refs. 12–14, 29, and 32, sample 1–3 in Ref. 30, and samples 2 and 4 in Ref. 31). It is found from the above cases that the influence of electron transfer on band bending is nearly neglected comparing to the contribution of gate voltage to band bending. However, for another case, the contribution of electron transfer to band bending should not be neglected since this contribution is unique to SIA of the quantum well in an illumination-controlled 2DEG system. For a quantum well

TABLE I. Layer structures of the studied samples.

	Sample 1	Sample 2	Sample 3
In _{0.53} Ga _{0.47} As cap layer	15 nm	15 nm	15 nm
In _{0.52} Al _{0.48} As	21 nm	25 nm	25 nm
Si δ doping	$5 \times 10^{12} \text{ cm}^{-2}$	$4 \times 10^{12} \text{ cm}^{-2}$	$4 \times 10^{12} \text{ cm}^{-2}$
In _{0.52} Al _{0.48} As spacer	4 nm	13.5 nm	12 nm
In _x Ga _{1-x} As channel	10 nm $x=0.53$	15 nm $x=0.60$	15 nm $x=0.65$
In _{0.52} Al _{0.48} As buffer	350 nm	350 nm	350 nm
Fe-doped Semi-insulating InP substrate (100)			

with δ doped only on one barrier, the band bending in the conductive channel should be enhanced due to the electrons transferring from the δ -doped layer to the channel after illumination. Thus, the SO coupling constant α should be increased and hence the zero-field spin-splitting energy $\Delta_0 = 2\alpha k_F$ (where k_F is the Fermi wave number) is also increased consequently due to the illumination either increasing the electron concentration.

In this work, the influence of illuminations on the beating patterns is discussed for three In_{0.52}Al_{0.48}As/In_xGa_{1-x}As/In_{0.52}Al_{0.48}As quantum-well samples with silicon δ doped on the upper barrier by means of magnetotransport measurements. It is observed that the beating nodes shift to lower and lower magnetic field after each illumination. The zero-field spin-splitting energy is found to decrease with increasing illumination, which is contrary to expectation. The electron concentration (Fermi wave number) dependence of spin-splitting energy contradicting the expectation may be due to the nonlinear Rashba spin-splitting mechanism.

II. EXPERIMENT

Three In_{0.52}Al_{0.48}As/In_xGa_{1-x}As/In_{0.52}Al_{0.48}As quantum-well samples were grown on semi-insulating InP(001) substrate using a GEN II solid-source molecular-beam-epitaxy system. The layer structures of the three samples are listed in Table I. The samples were cut by $5 \times 5 \text{ mm}^2$ square and four indium Ohmic contacts were made on each sample in a van der Pauw geometry. SdH measurements were performed using direct-current technique in a magnetic field range from 0 to 15 T and at different temperatures. The magnetic field is applied perpendicularly to the heterointerfaces. A red light-emitting diode was used to illuminate the samples at low temperature. After the samples are illuminated for each given time at low temperature, SdH measurements were performed once again to investigate the shift of the beating nodes. The 2DEG concentration is increased after each illumination. Due to the persistent photoconductivity effect, the increased 2DEG concentration persists for a long time, which is much longer than the time of the SdH measurements.

III. RESULTS AND DISCUSSION

Figure 1 shows the magnetoresistance ρ_{xx} of the 2DEG of sample 1 before and after illumination as a function of the applied magnetic field perpendicular to the heterointerface at

1.35 K, respectively. The beating nodes of SdH oscillations at low magnetic field are clearly observed [see the inset of Fig. 1(a) or Figs. 1(b) and 1(c)]. After illumination, the beating nodes shift to lower magnetic field. The beating patterns in Fig. 1 indicate the existence of two closely spaced frequency components of SdH oscillations with similar amplitudes. In order to obtain the frequencies of the oscillations,

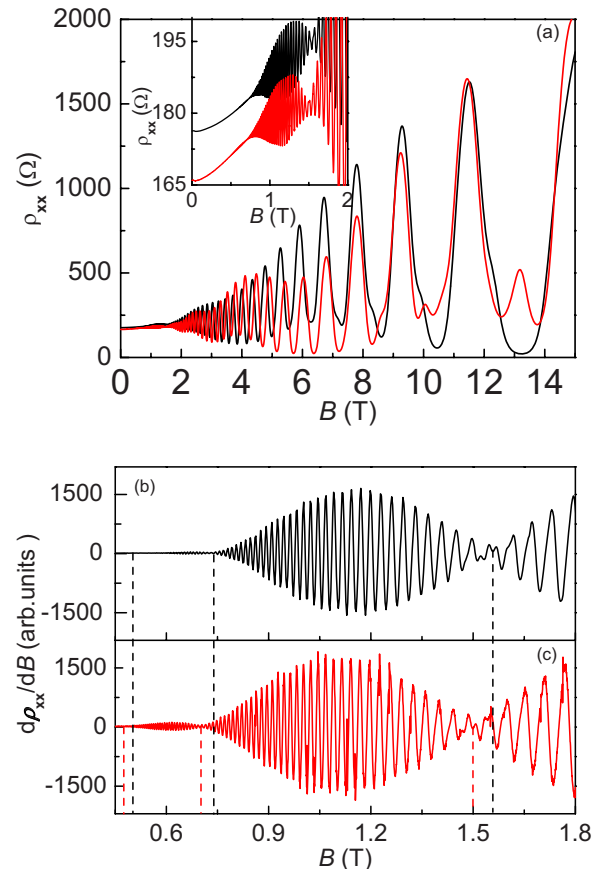


FIG. 1. (Color online) (a) The SdH oscillations of magnetoresistance ρ_{xx} of the 2DEG in sample 1 before (black line) and after (red line) illumination as a function of the applied magnetic field B perpendicular to the heterointerface at 1.35 K. The inset in (a) shows the beating patterns of the SdH oscillations before and after the illumination in low magnetic field range. In order to see the nodes position clearly, the first derivative of ρ_{xx} (b) before and (c) after illumination at 1.35 K is given. The vertical dash lines in (b) and (c) show the position of beating nodes.

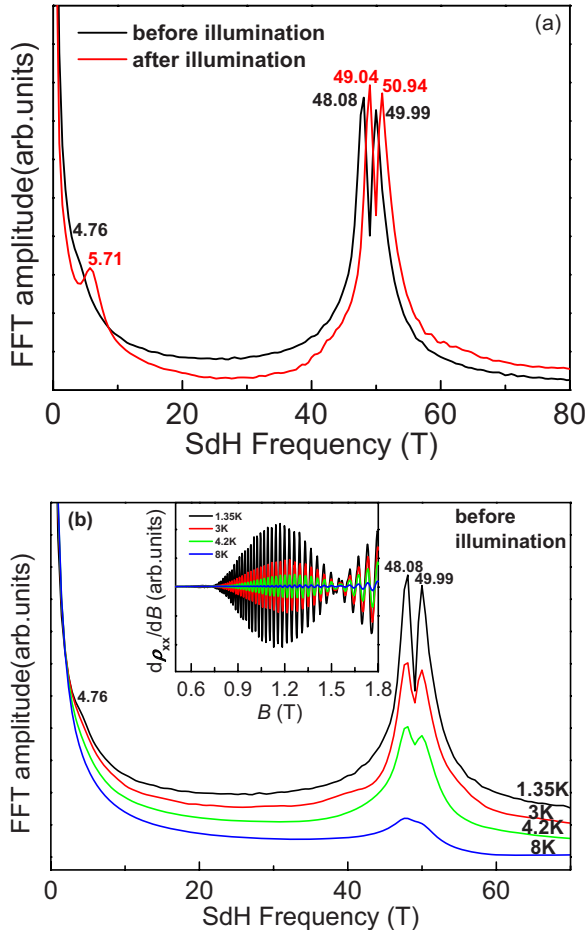


FIG. 2. (Color online) (a) FFT spectra of the magnetoresistance oscillations as a function of $1/B$ for sample 1 before and after the illumination at 1.35 K. (b) FFT spectra of the magnetoresistance oscillations as a function of $1/B$ for sample 1 before the illumination at various temperatures. FFT spectra both in (a) and (b) is taken with a magnetic field range between 0.4 and 2.5 T. The inset in (b) shows that the nodes positions in the SdH oscillations do not shift with increasing the temperature.

which are periodic in $1/B$, the fast Fourier transform (FFT) analysis is used. Figure 2(a) illustrates the FFT spectra of longitudinal resistance ρ_{xx} as a function of magnetic field at the temperature of 1.35 K, before and after illumination, respectively. FFT spectra of longitudinal resistance ρ_{xx} before illumination as a function of magnetic field at various temperatures are shown in Fig. 2(b). In order to tell that the beating nodes do not move when the temperature increases, the beating patterns of the first derivative of ρ_{xx} at different temperature are also shown in the inset of Fig. 2(b). Figure 2(a) indicates that the electron concentrations of both the first and the second subbands are enhanced after illumination. Whereas the second subband is slightly occupied by 2DEG and no spin splitting is observed. Hall electron concentrations $n_H = 2.61 \times 10^{12} \text{ cm}^{-2}$ and $2.72 \times 10^{12} \text{ cm}^{-2}$, and Hall mobilities $\mu_H = 1.40 \times 10^4 \text{ cm}^2/\text{Vs}$ and $1.38 \times 10^4 \text{ cm}^2/\text{Vs}$ for sample 1 before and after illumination are extracted from the experimental transversal resistance ρ_{xy} as a function of magnetic field and the conductance at zero magnetic field, respectively, at 1.35 K, and they are almost constant in the

measured temperature range. Due to the increase in the electron concentration and the decrease in mobility, the zero-field resistance is reduced slightly after the illumination [see the inset of Fig. 1(a)]. The electron effective mass of the 2DEG in sample 1 is $0.044 m_0$ (where m_0 is the free electron mass) obtained from the temperature dependence of the SdH oscillations before illumination and is almost unchanged after illumination.

The peaks of FFT spectra in Fig. 2(b) decrease rapidly when the temperature increases, indicating that the peaks do not derive from the magnetointersubbands scattering effect. Using $n = 2ef/h$,²⁶ the electron concentrations n before the illumination are calculated to be $2.32 \times 10^{12} \text{ cm}^{-2}$, $2.42 \times 10^{12} \text{ cm}^{-2}$, and $0.23 \times 10^{12} \text{ cm}^{-2}$ for the SdH frequencies f at 48.08, 49.99, and 4.76 T, respectively. And, the electron concentrations n after the illumination are calculated to be $2.38 \times 10^{12} \text{ cm}^{-2}$, $2.46 \times 10^{12} \text{ cm}^{-2}$, and $0.28 \times 10^{12} \text{ cm}^{-2}$ for the SdH frequencies f at 49.04, 50.94, and 5.71 T, respectively. The total electron concentration is exactly twice as high as the measured Hall concentration n_H , evidencing that the double-peak structure on the FFT spectra in Fig. 2 is due to the first subband splitting (left of spin degeneracy). Therefore, the electron concentrations n_{1+} , n_{1-} , and n_2 (n_{1+} , n_{1-} corresponding to the two spin-degenerated levels) are $1.21 \times 10^{12} \text{ cm}^{-2}$, $1.16 \times 10^{12} \text{ cm}^{-2}$, and $0.23 \times 10^{12} \text{ cm}^{-2}$ for the SdH frequencies f_{1+} at 49.99 T, f_{1-} at 48.08 T, and f_2 at 4.76 T for the sample before the illumination, and, are $1.23 \times 10^{12} \text{ cm}^{-2}$, $1.19 \times 10^{12} \text{ cm}^{-2}$, and $0.28 \times 10^{12} \text{ cm}^{-2}$ for the SdH frequencies f_{1+} at 50.94 T, f_{1-} at 49.04 T, and f_2 at 5.71 T for the sample after illumination, respectively. The total electron concentration including the spin-up and the spin-down subbands obtained from FFT analysis is almost equal to the measured n_H . The position of the FFT peaks almost do not change when the temperature increases [see Fig. 2(b)], also indicating that the electron concentration is almost constant in the measured temperature range.

We can extract estimates of the spin-splitting energy from the beating nodes since the above FFT analysis indicates that the beating nodes are induced by spin splitting of 2DEG. As discussed in Ref. 26, the spin-splitting Landau levels giving rise to two closely spaced frequencies with similar amplitudes lead to a modulation of the SdH amplitude

$$A \sim \cos \pi \nu, \quad (1)$$

where $\nu = \Delta / (\hbar \omega_c)$. Nodes in the beating pattern occur at half-integer values of ν ($\pm 0.5, \pm 1.5, \pm 2.5$, etc.). The last node corresponds to $\nu = 0.5$ and the successively lower nodes occur at $\nu = 1.5, 2.5, \dots$. The low magnetic field spin-splitting energies Δ at magnetic fields the nodes occur are determined according to the nodes position indicated in Figs. 1(b) and 1(c). By plotting the total spin splitting Δ as a function of magnetic field B , as shown in Fig. 3, the intercept of the extrapolation of the experimental Δ vs B with the vertical axis ($B = 0$) gives the zero-field spin-splitting energy $\Delta_0 = 3.81 \pm 0.01 \text{ meV}$ and $\Delta_0 = 3.57 \pm 0.01 \text{ meV}$ before and after illumination, respectively. It is indicated that the total zero-field spin-splitting decreases when the sample is illuminated because the illumination decreases the values of the magnetic field at the same ν [see Figs. 1(b) and 1(c)]. The

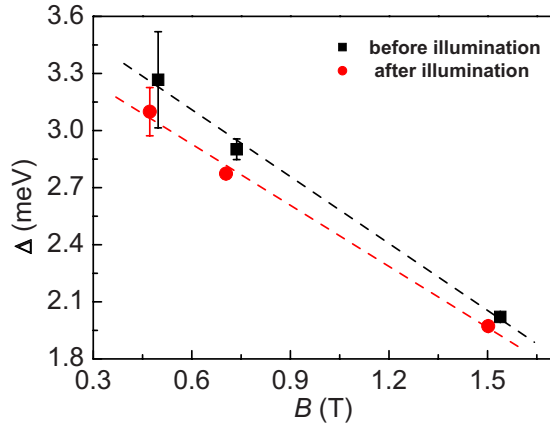


FIG. 3. (Color online) Total spin splitting for sample 1 at low field as a function of magnetic field B before and after the illumination. Line segments show the intercept used to determine Δ_0 .

Rashba SO coupling constant $\alpha = (4.94 \pm 0.01) \times 10^{-12}$ eV m and $(4.58 \pm 0.01) \times 10^{-12}$ eV m before and after the illumination are obtained according to the linear Rashba model $\Delta_0 = 2\alpha k_F$, respectively. It is truly believed that the illumination makes the reduction in the SO coupling constant despite the value of the SO coupling constant is weakened only about 7.3% if the linear Rashba model is applied since the illumination has enhanced the Fermi wave number of the spin resolved 2DEG from 3.86×10^8 to 3.90×10^8 m $^{-1}$ simultaneously while reduced the zero-field spin-splitting energy. Here we do not use the expression¹³ $\alpha = (\Delta n_1 \hbar^2 / m^*) [\pi / 2 (n_1 - \Delta n_1)]^{1/2}$ (where $n_1 = n_{1+} + n_{1-}$ and $\Delta n_1 = n_{1+} - n_{1-}$) and the obtained spin-resolved electron concentrations to determine the SO coupling constant α based on the fact that the additional contribution of the Zeeman term is included into the value of α though the FFT analysis is taken in a low magnetic field range.²²

For samples 2 and 3, the first measurement was performed before illumination at the temperature of 1.33 K. Next, the samples were illuminated for a short period of time and a second SdH measurement was performed after the illumination at the same temperature. After a longer and longer period of illumination followed by the previous SdH measurement, the same procedure was carried out repeatedly until no significant change in the data could be observed. The 2DEG concentration is increased after each given time illumination. In Figs. 4(a) and 4(b) we show the magnetoresistance ρ_{xx} of 2DEG for samples 2 and 3 as a function of the applied magnetic field at different electron concentration at 1.33 K, respectively. Figure 4 indicates that the beating nodes are shifted after each illumination. Same to the procedure applied to sample 1, the zero-field spin-splitting energy at different electron concentration of samples 2 and 3 can also be determined by analyzing the beating nodes. Figures 5(a) and 5(b) show zero-field spin-splitting energy as a function of Fermi wave number k_F of 2DEG for samples 2 and 3, respectively. The zero-field spin-splitting energy decreases with increasing the Fermi wave number k_F in the measured 2DEG concentration range for both samples.

For the samples, after illumination, some of the electrons of unactivated δ -doped silicon atoms (silicon-related DX

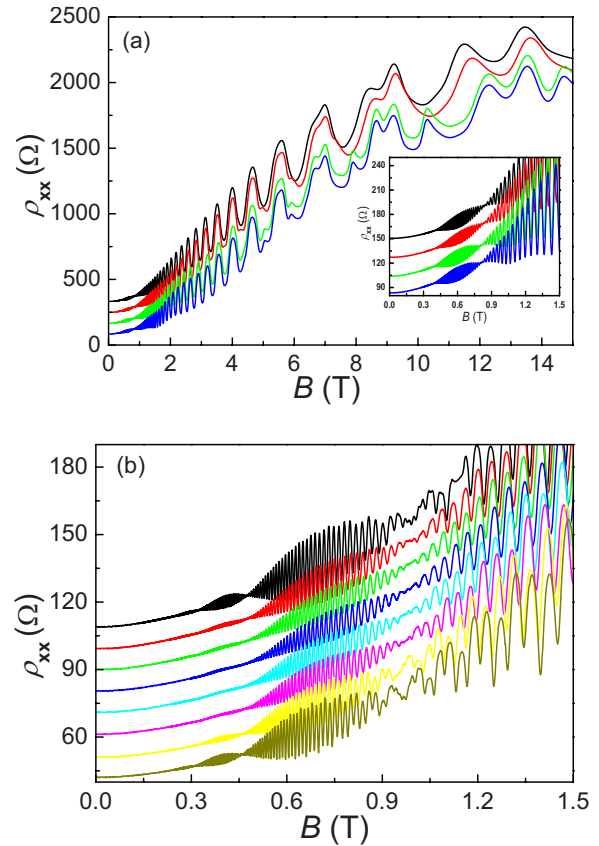


FIG. 4. (Color online) (a) The magnetoresistance ρ_{xx} of 2DEG for sample 2 as a function of the applied magnetic field at different electron concentration at 1.33 K. The inset shows the beating patterns of the SdH oscillations in low magnetic field range. (b) The beating patterns of the SdH oscillations of magnetoresistance ρ_{xx} for sample 3 in low magnetic field range at different electron concentration at 1.33 K. All the curves in (a) and (b) are vertically shifted for clarity. From top to bottom both in (a) and (b), the electron concentration is increased gradually.

centers) at the upper interface of $\text{In}_{0.52}\text{Al}_{0.48}\text{As}$ spacer layer are activated and then transfer into the quantum well while the residual positive charge centers still stay at the upper interface of the $\text{In}_{0.52}\text{Al}_{0.48}\text{As}$ spacer layer.³³ Therefore, the transfer increases the 2DEG concentration, and, the direction of the electric field induced by the electron transfer is positive to that in the quantum well, which should give rise to the enhancement of the quantum confinement of the quantum well. For $\text{In}_x\text{Ga}_{1-x}\text{As}/\text{In}_y\text{Al}_{1-y}\text{As}$ quantum wells, the dominant mechanism to the SO interaction is Rashba spin splitting.^{12,14,20,30} Though a relevant contribution to the linear Rashba SO coupling constant is governed by the band offset in the valence band and not by the macroscopic electric field alone evaluated from the bending of the conduction band,^{13,22,31,34} it was shown that the major contribution to the linear Rashba SO coupling constant originates from the band offset at the interface of the quantum well according to envelope function theory.²² Thus, the linear Rashba SO coupling constant is linearly dependent on the asymmetric conduction-band electric field $\langle F \rangle$ perpendicular to the 2DEG channel,¹² i.e., $\alpha = b\langle F \rangle$ [where b is inversely proportional to the energy gap of quantum well and the effective mass of

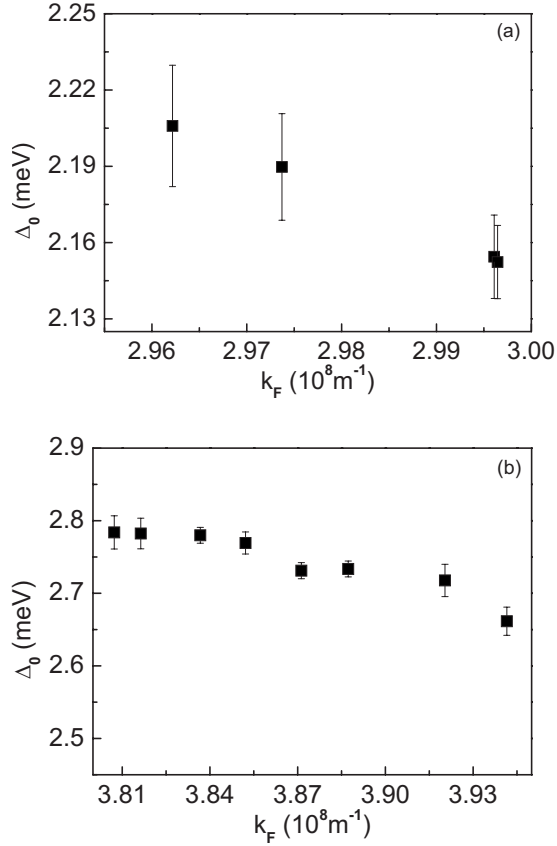


FIG. 5. Zero-field spin-splitting energy as a function of Fermi wave number k_F of 2DEG for (a) sample 2 and (b) sample 3.

2DEG (Ref. 17)]. The energy gap and the effective mass cannot be changed significantly by illumination, thus, the coefficient b is almost a constant. If the linear Rashba model satisfies the spin splitting, the SO coupling constant α should be increased at all time due to each illumination increases the average electric field in the well and hence the zero-field spin-splitting energy Δ_0 is always increased consequently due to the increase in the electron concentration after each illumination, which is contrary to the experimental results.

Some theoretical calculations indicated that the Rashba spin splitting in certain semiconductor quantum wells deviates from the linear behavior at large k_F (Refs. 21, 35, and 36) although the underlying physics is not clarified therein. It is indicated that the Rashba spin splitting is intrinsically a nonlinear function of the Fermi wave number.³⁷ The spin-splitting energy is described as $\Delta_0 = 2\alpha k_F / (1 + \beta k_F^2)$ (where α is the linear Rashba SO coupling constant for the above mentioned linear Rashba model $\Delta_0 = 2\alpha k_F$, βk_F^2 is due to the contribution of kinetic energy of electron).³⁷ According to the nonlinear Rashba model, the zero-field spin splitting can undergo a decrease tendency at large Fermi wave number though α increases with the average electric field in the well. In another words, the effective Rashba SO coupling constant $\alpha_e = \alpha / (1 + \beta k_F^2)$ not always increases with the increase in the average electric field in the well.

For the studied $\text{In}_{0.52}\text{Al}_{0.48}\text{As}/\text{In}_x\text{Ga}_{1-x}\text{As}/\text{In}_{0.52}\text{Al}_{0.48}\text{As}$ quantum wells here, the Fermi wave number is relatively large value. Thus, the zero-field spin splitting may transfer

into the range of nonlinear Rashba SO interaction. For the nonlinear Rashba model, the zero-field spin-splitting energy is dependent on α , β , and k_F , and $\alpha \propto \langle F \rangle / (E_g + E_0)$ and $\beta \propto 1/[m^*(E_g + E_0)]$ (where m^* is electron effective mass, E_g is the band gap of the quantum well, and E_0 is the quantum confining energy of the spin resolved subband).³⁷ Since the energy gap and the effective mass cannot be changed significantly by illumination or gate voltage, α increases with increasing the electric field $\langle F \rangle$ and decreasing the value of E_0 , and, β increases with decreasing the value of E_0 . Note that the decrease in E_0 implies the enhancement of the quantum confining energy, i.e., increasing the value of $E_F - E_0$. In experiment, it is not easy to observe the nonlinear Rashba spin splitting due to the competition α , β , and k_F . For a gate-controlled 2DEG system, the gate voltage change the band bending of conduction band, i.e., the electric field $\langle F \rangle$ along the quantum well prominently while changing the 2DEG concentration, i.e., the Fermi wave number k_F , thus it is more difficult to observe the nonlinear Rashba spin splitting. Whereas, the electric field $\langle F \rangle$ will not be change so prominently since the contribution of electron transfer to band bending is unique to SIA of the quantum well in an illumination-controlled 2DEG system. Therefore, the nonlinear Rashba spin splitting cannot be observed so difficultly. After each illumination, both α and β are altered due to the changes in the average electric field in the well and the position of the subband. Thus, we cannot determine α and β at each value of Fermi wave number k_F based on the relation of $\Delta_0 = 2\alpha k_F / (1 + \beta k_F^2)$. Furthermore, in Fig. 1 of Ref. 37, nonlinear Rashba spin-splitting energy can be illustrate as a function of Fermi wave number at a constant electric field $\langle F \rangle$ from numerical results of eight-band $k \cdot p$ theory. However, this situation cannot be found in practice since the electric field $\langle F \rangle$ always changes with the occupation of 2DEG, i.e., the Fermi wave number due to the occupation of 2DEG modifies the potential profile of energy band. So that α and β also cannot be determined directly by fitting the numerical results to the experimental one. Further study should be done to identify the nonlinear Rashba spin splitting both theoretically and experimentally.

IV. CONCLUSIONS

In summary, the beating patterns in the SdH oscillatory magnetoresistance originating from zero-field spin splitting of the 2DEGs in $\text{InGaAs}/\text{InAlAs}$ quantum wells have been investigated by means of magnetotransport measurements in the dark and after different illuminations. It is observed that the electron concentrations increase after each illumination. Meanwhile, the beating nodes induced by the zero-field spin-splitting effect shift to lower and lower magnetic field due to the decrease in the total zero-field spin splitting of the 2DEGs after each illumination. Since the transfer of electron by illumination enhances the electric field in the well, it is suggested that the total zero-field spin splitting of the 2DEGs in the $\text{In}_{0.52}\text{Al}_{0.48}\text{As}/\text{In}_x\text{Ga}_{1-x}\text{As}/\text{In}_{0.52}\text{Al}_{0.48}\text{As}$ quantum well arises from the nonlinear Rashba spin splitting, which was not reported previously by experiment. The nonlinear Rashba model needs be further developed to elucidate experimental

results and extract the correlative parameters.

ACKNOWLEDGMENTS

This work was supported by the Special Funds for Major State Basic Research Project (Grant No. 2007CB924900),

the National Natural Science Foundation of China (Grants No. 60906045, No. 60221502, and No. 60606025), the National Science Foundation for Post-doctoral Scientists of China (Grant No. 20070420634), and the Scientific Research Foundation of GuangXi University (Grants No. X071109 and No. XB2090777).

*zhouwz@mail.sitp.ac.cn

†jhchu@mail.sitp.ac.cn

- ¹S. Datta and B. Das, *Appl. Phys. Lett.* **56**, 665 (1990).
- ²J. Schliemann, J. C. Egues, and D. Loss, *Phys. Rev. Lett.* **90**, 146801 (2003).
- ³J. Nitta, F. E. Meijer, and H. Takayanagi, *Appl. Phys. Lett.* **75**, 695 (1999).
- ⁴T. Koga, J. Nitta, and M. van Veenhuizen, *Phys. Rev. B* **70**, 161302(R) (2004).
- ⁵X. Cartoixà, D. Z.-Y. Ting, and Y.-C. Chang, *Appl. Phys. Lett.* **83**, 1462 (2003).
- ⁶E. N. Bulgakov, K. N. Pichugin, A. F. Sadreev, P. Štředa, and P. Šeba, *Phys. Rev. Lett.* **83**, 376 (1999).
- ⁷T. Koga, J. Nitta, H. Takayanagi, and S. Datta, *Phys. Rev. Lett.* **88**, 126601 (2002).
- ⁸J. I. Ohe, M. Yamamoto, T. Ohtsuki, and J. Nitta, *Phys. Rev. B* **72**, 041308(R) (2005).
- ⁹G. Dresselhaus, *Phys. Rev.* **100**, 580 (1955).
- ¹⁰E. I. Rashba, *Sov. Phys. Solid State* **2**, 1109 (1960).
- ¹¹Y. A. Bychkov and E. I. Rashba, *J. Phys. C* **17**, 6039 (1984).
- ¹²J. Nitta, T. Akazaki, H. Takayanagi, and T. Enoki, *Phys. Rev. Lett.* **78**, 1335 (1997).
- ¹³G. Engels, J. Lange, Th. Schäpers, and H. Lüth, *Phys. Rev. B* **55**, R1958 (1997).
- ¹⁴C. M. Hu, J. Nitta, T. Akazaki, H. Takayanagi, J. Qsaka, P. Pfeffer, and W. Zawadzki, *Phys. Rev. B* **60**, 7736 (1999).
- ¹⁵D. Grundler, *Phys. Rev. Lett.* **84**, 6074 (2000).
- ¹⁶J. P. Lu, J. B. Yau, S. P. Shukla, M. Shayegan, L. Wissinger, U. Rössler, and R. Winkler, *Phys. Rev. Lett.* **81**, 1282 (1998).
- ¹⁷G. Lommer, F. Malcher, and U. Rössler, *Phys. Rev. Lett.* **60**, 728 (1988).
- ¹⁸J. Luo, H. Munekata, F. F. Fang, and P. J. Stiles, *Phys. Rev. B* **38**, 10142 (1988).
- ¹⁹J. Luo, H. Munekata, F. F. Fang, and P. J. Stiles, *Phys. Rev. B* **41**, 7685 (1990).
- ²⁰B. Das, S. Datta, and R. Reifenberger, *Phys. Rev. B* **41**, 8278 (1990).
- ²¹E. A. de Andrada e Silva, G. C. La Rocca, and F. Bassani, *Phys. Rev. B* **50**, 8523 (1994).
- ²²Th. Schäpers, G. Engels, J. Lange, Th. Klocke, M. Hollfelder, and H. Luth, *J. Appl. Phys.* **83**, 4324 (1998).
- ²³P. Pfeffer and W. Zawadzki, *Phys. Rev. B* **52**, R14332 (1995).
- ²⁴P. Pfeffer, *Phys. Rev. B* **55**, R7359 (1997).
- ²⁵P. Pfeffer and W. Zawadzki, *Phys. Rev. B* **59**, R5312 (1999).
- ²⁶B. Das, D. C. Miller, S. Datta, R. Reifenberger, W. P. Hong, P. K. Bhattacharya, J. Singh, and M. Jaffe, *Phys. Rev. B* **39**, 1411(R) (1989).
- ²⁷Y. S. Gui, C. M. Hu, Z. H. Chen, G. Z. Zheng, S. L. Guo, J. H. Chu, J. X. Chen, and A. Z. Li, *Phys. Rev. B* **61**, 7237 (2000).
- ²⁸W. Z. Zhou, T. Lin, L. Y. Shang, G. Yu, Z. M. Huang, S. L. Guo, Y. S. Gui, N. Dai, J. H. Chu, L. J. Cui, D. L. Li, H. L. Gao, and Y. P. Zeng, *Solid State Commun.* **143**, 300 (2007).
- ²⁹V. A. Guzenko, Th. Schäpers, and H. Hardtdegen, *Phys. Rev. B* **76**, 165301 (2007).
- ³⁰T. Koga, J. Nitta, T. Akazaki, and H. Takayanagi, *Phys. Rev. Lett.* **89**, 046801 (2002).
- ³¹Y. P. Lin, T. Koga, and J. Nitta, *Phys. Rev. B* **71**, 045328 (2005).
- ³²G. Yu, N. Dai, J. H. Chu, P. J. Poole, and S. A. Studenikin, *Phys. Rev. B* **78**, 035304 (2008).
- ³³W. Desrat, D. K. Maude, Z. R. Wasilewski, R. Airey, and G. Hill, *Phys. Rev. B* **74**, 193317 (2006).
- ³⁴R. Winkler, S. J. Papadakis, E. P. De Poortere, and M. Shayegan, *Adv. Solid State Phys.* **41**, 211 (2001).
- ³⁵R. Winkler and U. Rössler, *Phys. Rev. B* **48**, 8918 (1993); R. Winkler, *ibid.* **62**, 4245 (2000).
- ³⁶S. Lamari, *Phys. Rev. B* **64**, 245340 (2001).
- ³⁷W. Yang and Kai Chang, *Phys. Rev. B* **74**, 193314 (2006).